The 2010 IEEE/RSJ International Conference on
Intelligent Robots and Systems
October 18-22, 2010, Taipei, Taiwan

Adaptive Multi-dimensional Compliance Control of a Humanoid Robotic Arm with Anti-Windup Compensation

Said G Khan, Guido Herrmann, Tony Pipe and Chris Melhuish

Abstract— **An adaptive multi-dimensional compliance model reference controller was implemented in real-time on a 4 degrees of freedom (DOF) of the humanoid Bristol-Elumotion-Robotic-Torso II (BERT II) arm in Cartesian space. The robot manipulator has been controlled in such a way as to follow the compliant passive behaviour of a reference mass-spring-damper system model subject to externally sensed forces/torques in all DOF. The relevant reference model converts all measured torques into their equivalent forces at the end-effector and reacts accordingly. The suggested control scheme takes in particular account of the multi-variable aspect and the problem of body own torques when measuring external torques. The redundant DOF were used to control the robot motion in a human-like pattern via effort minimization. Associated actuator saturation issues were addressed by incorporating a novel anti-windup (AW) compensator.**

I. Introduction

Human-robot physical interaction is one of the most important scenarios of human-robot cooperation. Human safety is at the core of human-robot cooperation and interaction. Compliance control can help in achieving safe human-robot interaction. There are two options for compliance, passive compliance and active compliance. Passive compliance is based on a suitable robot mechanical build, which avoids physical injury at impact or due to other interacting forces. However, passive compliance cannot be used in our case. This is due to the fact that our BERT II robotic arm is inherently rigid.

In our case, an active compliance control scheme has therefore been used to make it safer for interaction with humans. The torque sensors installed in the robot joints have been used to implement the scheme. Active compliance has been investigated by various researchers to deal with the safety aspects of human-robot interaction some of the related work can be found in [1] - [10].

Often compliance or impedance controllers are model-based nonadaptive schemes, e.g. [1], [3], [5], [8], [11] - [14].

However, for a large scale multi-redundant robot system, exact identification is rather complex. Component ageing or damage may invalidate these dynamics identifications. Hence, it is preferred here to use adaptive schemes which can guarantee predesigned passive characteristics in the face of a changing system.

In general, there are two main types of adaptive control schemes i.e. *model reference adaptive control (MRAC)* and *self tuning (ST)* adaptive control. In MRAC, the adaptation mechanism works, so that the plant response becomes the same as that of a reference model (see [15]). The reference model in our case is a second order mass-spring-damper system.

The authors of [16]-[18] (see also [19] for an advanced formulation) have suggested two model free adaptive compliant control schemes for rigid link manipulators. The first one is an adaptive impedance controller. In this approach, the impedance of the end effector is ensured via an MRAC scheme guaranteeing a passive reference system. The second scheme is an adaptive position/force controller in which the end effector's space is separated into the direction in which the end effector can move and the direction it is exerting force. The controller then ensures the desired values of force and position in the corresponding directions.

The main control strategy applied in this paper is a model reference adaptive compliance controller (see [17]). The main controller is augmented by an additional effort minimizing 'posture' controller. This 'posture' controller controls the redundant DOF via minimization of an effort function (which is a function of gravity and will be defined later in this paper) to achieve human like motion based on the work of [20]-[22].

Aspects of the problem of sensing external torques via robot body-internal torque sensors are suitably addressed by estimating the major body own torques first to extract external torques. Moreover, the control scheme presented by [17] is adjusted to allow for a more versatile set of controller parameters suited to the multi-variable control problem of multi-redundant robots.

The adaptive controller does not account for actuator saturation, causing windup of the adaptation algorithm. To avoid this, an AW compensation system given in [23] has been employed for the scheme of [17].

Based on the comments above, the paper provides the following contributions:

- Extension of the adaptive compliance controller scheme from [17], to allow for better multi-variable control performance.
- Extending the controller to include an AW compensator to make it safer, as without it, the controller will destabilize because of actuator saturation.
- Inclusion of a posture torque controller to generate human like motion.
- Successful implementation of the scheme on a real system (humanoid BERT II arm).

II. Adaptive Compliance Control

The MRAC adaptive controller developed by [17]; has been employed and extended here by an AW-compensation scheme while the controller scheme has been suitably modified to improve multi-variable control performance. The

scheme is similar to our recent work [24]. Where, a one dimensional compliance control scenario was investigated while in this paper a multi-dimensional compliance scenario has been considered. We assume the general structure of the robot dynamics is given by:

$$M(q)\ddot{q} + V(q,\dot{q}) + G(q) = T \tag{1}$$

where *M* is the inertia matrix, a function of the n joint angles q. V is the coriolis/centripetal vector, which also represents viscous and nonlinear damping. G is the gravity vector. T is the input torque. The Cartesian space dynamics are now given as follows: Instead of joint torques, the dynamics equate to the forces, acting on the end effector:

$$A(q)\ddot{X} + \mu_{cc}(q,\dot{q}) + f(q) = F \tag{2}$$

where $A = (JM^{-1}J^T)^{-1}$, $\mu_{cc} = \bar{J}^T V - A\dot{J}\dot{q}$, $f = \bar{J}^T G$, $F = \bar{J}^T T$ and X is the robot end-effector Cartesian position, i.e. $[x, y, z]^T$, and J is the Jacobian of the robot arm's kinematics.

Cartesian velocities are defined as $\dot{X} = J\dot{q}$. The matrix $\bar{J}$ is the inertia weighted pseudo Jacobian inverse is given by $\bar{J} = M^{-1}J^T(JM^{-1}J^T)^{-1}$ [25], (see also [26]).

The Cartesian position of the end effector is used here to define the motion task of the robot. Hence, the dynamics of (2) represent here the Cartesian or Task dynamics. The adaptive Cartesian/task control law is:

$$F = \hat{A}\ddot{X}_d^* + \hat{B}\dot{X}_d^* + \hat{f} + F_{ext} + [2k + \hat{K}]r \tag{3}$$

where, $\hat{A}$, $\hat{B}$, $\hat{f}$ and $\hat{K}$ are adaptive gains given later, while k is a positive scalar constant chosen by the designer. Moreover, the modified velocity and acceleration error are given by $\dot{X}_d^* = \dot{X}_d + \Lambda e_x$ and $\ddot{X}_d^* = \ddot{X}_d + \Lambda \dot{e}_x$ respectively. The Cartesian position error is given by $e_x = X_d - X$, where X_d the Cartesian demand position derived from a reference model, to be discussed later. The demand position X_d is the result of the reference model discussed later in this section. The vector r is the filtered error and is defined as: $r = \dot{e}_x + \Lambda e_x$ and Λ is a 3×3 diagonal matrix with positive values. The adaptive law estimating the gravity vector is given as:

$$\dot{\hat{f}} = -K_{\alpha_1}\hat{f} + K_{\beta_1} r \tag{4}$$

The inertia matrix in Cartesian coordinates is estimated in:

$$\dot{\hat{A}} = -K_{\alpha_2}\hat{A} + K_{\beta_2} r(\ddot{X}_d^*)^T \tag{5}$$

Coriolis/Centripetal forces are indirectly estimated via the matrices $\hat{B}$ and $\hat{K}$:

$$\dot{\hat{B}} = -K_{\alpha_3}\hat{B} + K_{\beta_3} r(\dot{X}_d^*)^T \tag{6}$$

$$\dot{\hat{K}} = -K_{\alpha_4}\hat{K} + K_{\beta_4} r r^T \tag{7}$$

using the following dynamically changing forgetting factor: $K_{\alpha_i} = K_{\alpha_{i0}} + K_{\alpha_{i1}}||\dot{X}||$ with the assumption that K_{β_i}, $K_{\alpha_{i0}}$ and $K_{\alpha_{i1}}$ are positive definite diagonal matrices with $i = 1-4$. Note the minor but practically important difference of using diagonal gains for the adaptation laws in difference to [17]. This allows for better tracking of multi-variable

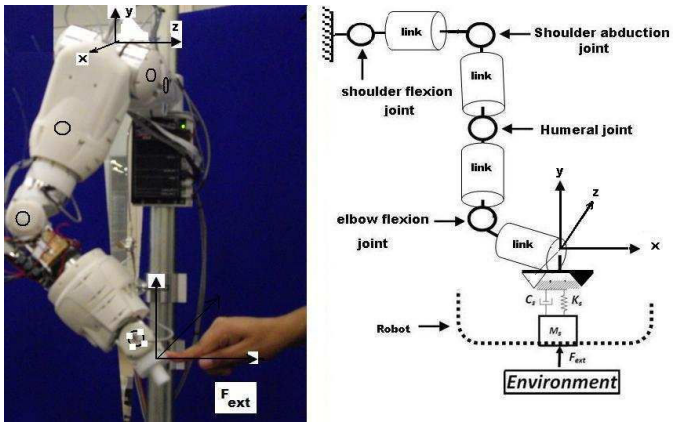

Fig. 1. Robot interacts with the environment like a spring mass damper system.

control performance in contrast to [17]. The applied torque for adaptive control is: $T = J^T F$ which is sufficient to control the Cartesian/task dynamics (2). Nevertheless, the dynamics of (2) represent only three degrees of freedom and other control terms have to be augmented to retain stability of the other $(n-3)$ degrees of freedom, representing the posture or null-space dynamics in relation to the task dynamics.

The reference impedance model characteristics are defined by the mass matrix M_s, the damping coefficient matrix C_s and the stiffness coefficient matrix K_s. These values determine the behaviour of the reference model:

$$M_s\ddot{X}_d + C_s\dot{X}_d + K_s X_d = -F_{ext} + M_s\ddot{X}_r + C_s\dot{X}_r + K_s X_r \tag{8}$$

where, F_{ext} is the external Cartesian forces sensed through the joint torque sensors , X_r is the reference trajectory and X_d is the new demand to compensate the external forces. Hence, M_s, C_s and K_s can be used to adjust the level of compliance. As the main control approach is applied to a multi-redundant system, the motion is under-constrained, and some links may follow bounded but seemingly random trajectories for a Cartesian demand position. Therefore, a posture torque controller has been added which deals with the redundant motion, to generate a human like movement pattern by minimizing the effort (a function of gravity) during reaching to a particular point in the robot work space. The method here is adopted from previous work by [20], [21] (see also [22]). The 'posture' controller T_p is in the null space of the adaptive Cartesian controller, hence, it does not affect the main controller:

$$T = J^T F + N^T T_p,\ N^T = (I - J^T\hat{\bar{J}}^T) \tag{9}$$

where I is the identity matrix. $\hat{\bar{J}}$ is the preliminary estimate of the inertia weighted pseudo Jacobian inverse defined earlier. The posture torque, T_p is calculated in the same way as given in [20], [21] and [24] by minimizing the joint effort function $U_p = G^T(K_m)^{-1}G$, where, G is the gravitational vector term from equation (1), and K_m is the actuator activation matrix, having positive diagonal elements.

III. Anti-Windup Compensator

Due to the highly dynamic character of the adaptive control scheme, actuators can become saturated. This has shown to cause windup of the adaptation algorithms (4)-(7), causing destabilization of the robot controller, creating a highly unsafe environment for humans. Hence, a suitable avoidance of the windup of the adaptation algorithms guarantees the controller performance in case of saturation. Another important aim is to recover nominal adaptive control performance, once the actuator saturation is overcome. Therefore, an AW compensator system is adopted from [23], originally developed for a neural network control scheme. Two functions $DZ_{K_f}(||F||)$ and $c(DZ_{K_f}(||\bar{F}||))$ are introduced for this anti-windup compensator:

$$DZ_{K_f}(||F||) = \begin{cases} ||F|| - K_f, & if||F|| > K_f \\ 0, & if||F|| \leq K_f \end{cases} \quad (10)$$

K_f is the artificial limit, imposed on the control signal. The function $c(\cdot)$, $0 \leq c \leq 1$ is a smooth scheduling element defined as follows,

$$c(DZ_{K_f}) = \frac{K_f^2 \delta}{(K_f + DZ_{K_f})(K_f \delta + DZ_{K_f})} \quad (11)$$

where δ is a positive design constant. The purpose of scheduling element c is to activate a sliding mode element when actuator saturation is foreseen due to large amplitudes in F. When $c = 1$, only the adaptive controller is active and if $c = 0$, only a sliding mode control is active. If $0 < c < 1$, both adaptive and sliding mode controllers are active, each at a reduced level. Using $c(DZ_{K_f}(||F||))$ and $DZ_{K_f}(||F||)$ the adaptation laws for $\hat{A}$, $\hat{B}$, $\hat{f}$ and $\hat{K}$ are modified online. The adaptive law estimating the gravity forces becomes then:

$$\dot{\hat{f}} = -K_{\alpha_1} \hat{f} + K_{\beta_1} cr \quad (12)$$

Similarly, the adaptive law estimating the inertia matrix is modified to:

$$\dot{\hat{A}} = -K_{\alpha_2} \hat{A} + K_{\beta_2} cr(\ddot{X}_d^*)^T \quad (13)$$

$$\dot{\hat{B}} = -K_{\alpha_3} \hat{B} + K_{\beta_3} cr(\dot{X}_d^*)^T \quad (14)$$

$$\dot{\hat{K}} = -K_{\alpha_4} \hat{K} + K_{\beta_4} crr^T \quad (15)$$

Equation (14) and (15) are the modified form of the adaptive laws indirectly estimating coriolis/centripetal forces while the forgetting factors are modified to:

$$K_{\alpha_i} = K_{\alpha_{i0}} + K_{\alpha_{i1}} ||\dot{X}|| + K_{\alpha_{i2}} DZ_{K_f} \quad (16)$$

where $K_{\alpha_{i2}}$ are positive definite diagonal design matrices. Note that the adaptation laws of (13)-(15) are now also including c in contrast to (4)-(7). This modifies for $c \rightarrow +0$ the adaptive laws into autonomous asymptotically stable systems so that windup prevention is introduced, which is enhanced by the increase of the forgetting factor in (16). Using this modified adaptive law, this changes the control law to:

$$\hat{F} = cF + (1 - c) K_f \frac{r}{||r||} \quad (17)$$

and the applied torques are now:

$$T = Sat(J^T \hat{F} + (I - J^T \hat{\bar{J}}^T) T_p) \quad (18)$$

where, $Sat(\cdot)$ is the saturation function defined by the amplitude limits of the actuators and $\hat{\bar{J}}$ accounts for the uncertain $\hat{M}$. The argument of the function $c(DZ_{K_f}(||F||))$ has been omitted in the equations above using only c. Note that K_f has to be chosen so that $J^T \hat{F}$ remains strictly within the linear region of $Sat(\cdot)$, considering $J^T \hat{F}$ as the argument. A block diagram of the overall control scheme is shown in Figure 2.

The anti-windup compensator significantly enlarges the region of attraction of the control system in contrast to the adaptive control scheme alone, which destabilizes, once the control signal is saturated due to the adaptive control scheme. This is avoided by introducing an amplitude limited sliding mode element which replaces the adaptive scheme until the magnitudes of $\hat{f}$, $\hat{A}$ and $\hat{K}$ have recovered to smaller values.

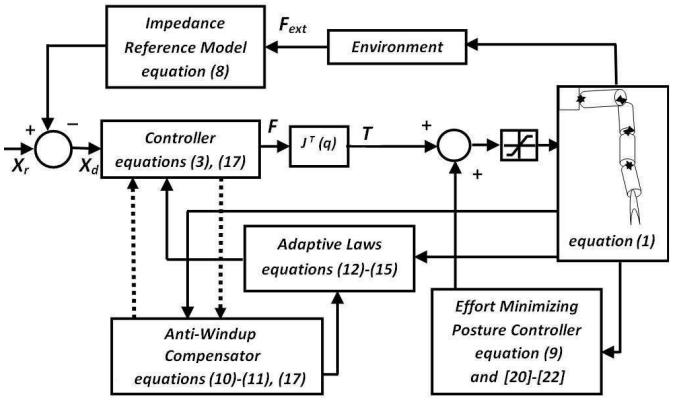

Fig. 2. Model reference adaptive compliance controller with AW compensator and effort minimizing controller.

IV. Results & Discussion

As mentioned, the BERT II arm has 7 DOF, however, only 4 DOF namely, shoulder flexion, shoulder abduction, humeral rotation and elbow flexion are used as shown in Figure 1. The base coordinate frame is fixed in the shoulder. The end effector position is specified with respect to the base frame.

A. Joints Torque Sensors and Body Toques estimates

As mentioned before, the BERT II arm is equipped with torque sensors in each joint to measure the external applied forces/torques. These sensors are strain gauges arranged in a wheatstone bridge. Torque sensors were experimentally calibrated by hanging different weights and recording voltage change. When there are no external forces/torques, the joint torque sensors measure the gravity torques $T_G \; \varepsilon \Re^{4\times 1}$ (plus also Coriolis/centripetal force if the robot arm is moving). However, at lower velocities, coriolis/centripetal torques will be very small as compared to gravity torques. It is necessary to compensate for these body inherent torques when measuring external torques and forces. This is achieved by posing

the gravity torque as a linear parameterized expression:

$$T_G = \hat{\phi} W(q) \tag{19}$$

where $\hat{\phi}\ \varepsilon \Re^{4\times 6}$ contains the parameter estimates depending on the robot and the sensors scale, while $W\ \varepsilon \Re^{6\times 1}$ is the regressor function formed by the geometric nonlinearities of the robot. Thus, W is a matrix consisting of suitable sin/cos functions. The parameter matrix $\hat{\phi}$ is estimated during an initial test period using a recursive least square algorithm minimizing $\sum_i \parallel T_{Gi} - \hat{T}_{Gi} \parallel^2$, $\hat{\phi}$ is constant during normal operation. As a result, the actual body torques (T_G) and their estimates ($\hat{T}_G$) are shown in Figure 3. These estimates of the gravity torques allows differentiating of external torques T_{ext} from body-own torques of the robot: $\hat{T}_{ext} = T_{measured} - T_G$

In fact, we are using $T_{ext} = Dz(T_{measured} - T_G)$, where, Dz is the dead zone function, to avoid the small errors in T_G affecting T_{ext}. The external torques, T_{ext}, result from external forces, F_{ext}, acting on the end-effector of the robot in $x - y - z$ coordinates. Thus, the external torques T_{ext} have to be mapped to these forces, F_{ext}, using the inverse of Jacobian J defined earlier. Note that J is not invertible and it has been found that the pseudo inverse in this case gives numerically wrong results for certain poses, giving incorrect, large amplitudes for the estimated values F_{ext}. Similarly, it was found that the damped pseudo-inverse $J^T(JJ^T + \rho^2 I)^{-1}$ also gives large errors when computing, F_{ext} in some cases. The most suited approximate inverse in our case is the inverse using singular value decomposition (SVD): $J = USV^T$, where U and V are unitary (possibly non square) matrices and S is a matrix, where only the diagonal values are nonzero, holding *only* the non-negative singular values of J. The SVD based Jacobian inverse is: $J^{-1}_{SVD} = VS^{-1}U^T$ Hence, the estimated end-effector Cartesian forces are: $F_{ext} = J^{-T}_{SVD} T_{joints}$

B. Tracking and Compliance Results

Good tracking can be observed in experiments on the real robot as shown in Figure 4. In this experiment on the real BERT II arm, the end-effector was moved in a circle in the $X - Z$ plane by giving a sine wave position demand to z and cosine wave position demand to x.

In the absence of external forces, the robot end-effector should follow the reference trajectory X_r. In the presence of external contact forces the reference trajectory is modified for X_d and the robot will follow this new demand trajectory defined by the impedance reference model (8) to compensate for the external forces.

The MRAC-approach allows us to design well-defined levels of compliance for safe human-robot interaction by choosing the correct values for the parameters K_s and C_s for $x - y - z$ direction. Thus, it was tested for different stiffness and damping values imposed via the model reference given in equation (8), for external contact forces. The results produced in an experiment when external forces in $x - y - z$ were applied by pushing and pulling the robot end-effector while using different values of K_s and C_s, two of the experiments

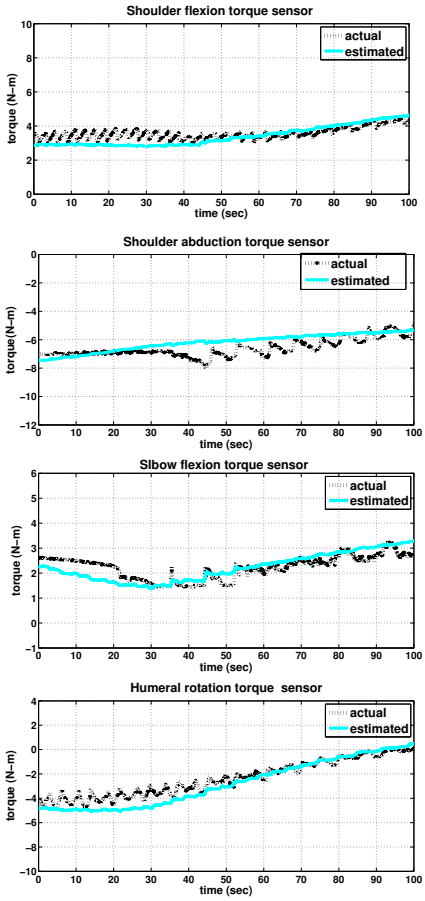

Fig. 3. Robotic arm's body torques estimates, T_G, $\hat{T}_G$.

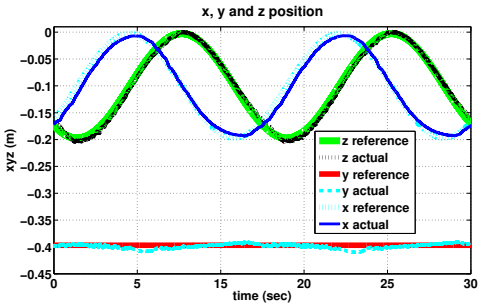

Fig. 4. Cartesian position x (for a cosine demand), y (for a constant demand) and z (for a sine demand).

are shown in Figures 5-6. The end-effector trajectory follows the demanded reference model trajectory nicely.

C. Anti-windup Compensator results

Practical tests have shown that without an AW compensator, actuator amplitude limits of $\pm 3000mA$ are reached and the control system becomes easily unstable. Inclusion of the AW compensator prevents instability due to saturation. As mentioned previously, the scheduling element $c = 1$ means that the adaptive scheme is only active (see equation (17)). If $c = 0$, the sliding mode element alone is active, if $0 < c < 1$, then both the sliding mode and the adaptive controller are active. For the real robot, it is seen that the adaptive controller is operating for most of the time, while the sliding mode scheme is only used over a short span of time when any of the actuators reaches its amplitude limit. This is

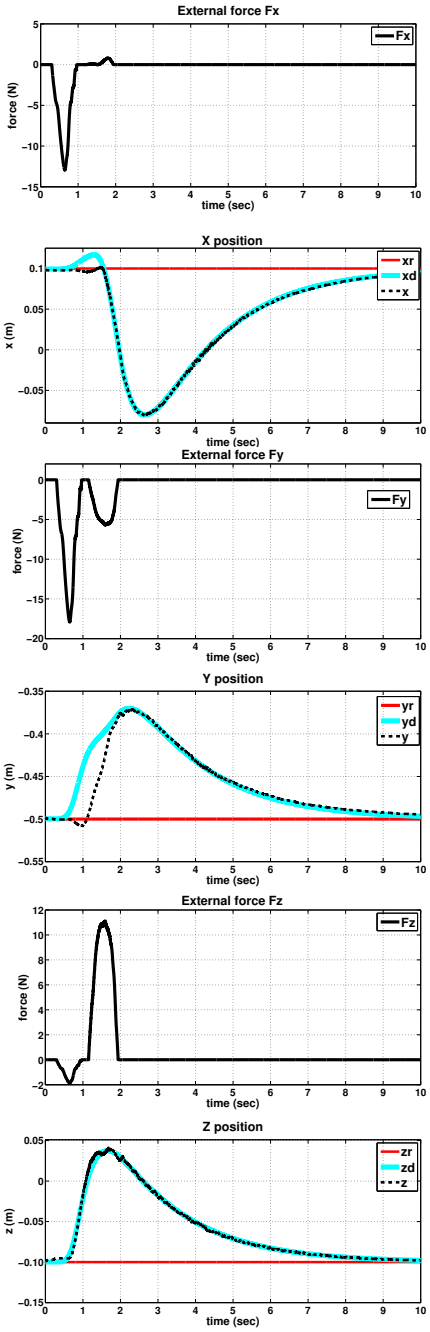

Fig. 5. Cartesian position x, y and z, when external contact forces act for $Ksxz = 10N/m$, $Csxz = 20Ns/m$, $Ksy = 20N/m$, $Csy = 40Ns/m$ and with $Msxyz = 2Kg$.

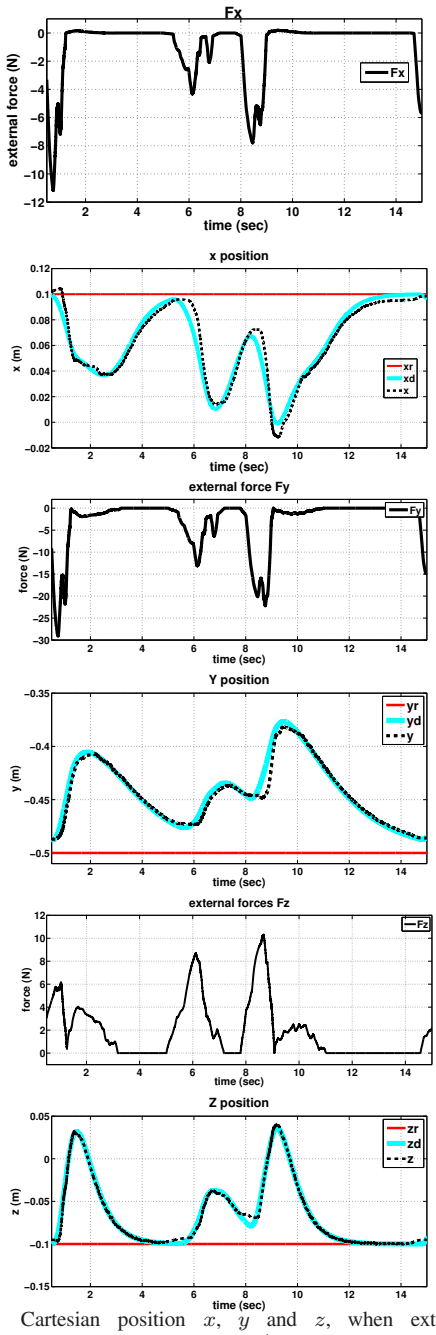

Fig. 6. Cartesian position x, y and z, when external contact forces(Cartesian) act for $K_{sxz} = 50N/m$, $C_{sxz} = 30Ns/m$, $K_{sy} = 30N/m$, $C_{sy} = 100Ns/m$) and with $Msxyz = 2Kg$.

particularly observed in Figure 7 for the scheduling element c which remains most of the time at $c = 1$. Hence, the AW scheme is effective, avoiding instability due to saturation but also recovering the nominal adaptive controller performance. Figure 7 also shows the motor current inputs of the humeral rotation joint and the shoulder flexion joint, which stay within the actuator amplitude limits of $\pm 3000mA$. The other two actuators (elbow flexion and shoulder abduction) are not shown, as in this experiment, their amplitude remained well below their amplitude limit. Note that this AW scheme also adds to the safety of the control scheme as it allows for the adaptive scheme to operate in the nominal case, while the AW scheme returns control to the case without saturation as quickly as possible, avoiding stability and performance loss in case of actuator saturation.

V. Conclusion

In this paper, we have focused on a practical active multi-dimensional compliance control technique for achieving safety in the face of human-robot physical interaction. We have shown that multi-dimensional compliance and flexibility can be achieved with some acceptable compromises in accuracy. The redundant DOF has been used to generate human like motion by minimizing muscle(actuator) effort(which is a function of gravity). In particular, we have been able to

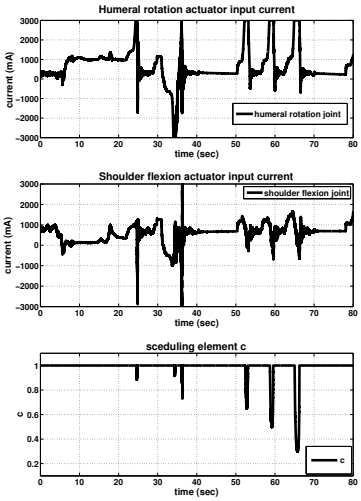

Fig. 7. Shoulder flexion and humeral rotation joint input currents are pushed to stay inside the actuator amplitude limits, scheduling element $c(\cdot)$ is also shown.

design different levels of compliance, which is important for the different situations of human-robot interaction that could occur in the real world. AW compensator has been added to deal with the actuators saturation caused by adaptive controller, which increases safety by avoiding instability caused by actuators saturation.

VI. Acknowledgements

The research leading to these results has received funding from the European Community's Information and Communication Technologies Seventh Framework Programme [FP7/2007-2013] under grant agreement no. [215805], the CHRIS project. Please see, "www.chrisfp7.eu".

References

[1] S. Komada and K. Ohnishi, "Robust force and compliance control of robotics manipulators," in *Proceedings of the International Conference on Industrial Electronics*, Hyatt Regency, Singapore, October 1988.

[2] Z. Peng and N. Adachi, "Compliant motion control of kinematically redundant manipulators," *IEEE Transactions on Robotics and Automation*, vol. 9, pp. 831–837, Febuarary 1993.

[3] B. Shetty and M. Ang, "Active compliance control of a puma 560 robot," in *Proceedings of the IEEE International Conference on of Robotics and Automation*, Minneapolis, Minnesota, Canada, 1996.

[4] M. Al-Jarrah and Y. Zheng, "Intelligent compliant motion control," *IEEE Transaction on System, Man, and Cybernetics-Part B Cybernetics*, vol. 28, pp. 116–122, Febuarary 1998.

[5] C. Albrichsfeld and H. Tolle, "A self-adjusting active compliance controller for multiple robots handling an object," *Control Engineering Practice*, vol. 10, pp. 165–173, February 2002.

[6] T. Tsumugiwa, R. Yokogawa, and K. Hara, "Variable impedance control based on estimation of human arm stiffness for human-robot cooperative calligraphic task," in *Proceedings of the IEEE International Conference on Robotics*, Washington,USA, May 2002, pp. 644–650.

[7] L. Zollo, S. B., C. Laschi, G. Teti, and P. Dario, "An experimental study on compliance control for a redundant personal robot arm," *Robotics and Autonomous Systems*, vol. 44, pp. 101–129, 2003.

[8] A. Bichi and G. Tonietti, "Design, realization and control of soft robot arms for intrinsically safe interaction with humans," in *Proc. IARP/RAS Workshop on Technical Challenges for Dependable Robots in Human Environments*, October 2002, pp. 79–87.

[9] W. Zhang, Q. Huang, P. Du, J. Li, and K. Li, "Compliance control of a humanoid arm based on forced feedback," in *Proceedings of the 2005 IEEE International Conference on Information Acquisition*, Hong Kong and Macau, China, July 2005.

[10] D. Formica, L. Zollo, and Gulielmelli, "Torque-dependent compliance control in the joint space of an operational robotic machine for motor therapy," in *Proceedings of the 2005 IEEE 9th International Conference on Rehabilitation Robotics*, Chicago, IL, USA, June 2005, pp. 341–344.

[11] A. Albu-Schäffer, Haddadin, C. Ott, T. Stemmer, G. Wimbck, and Hirzinger, "The dlr lightweight robot: design and control concepts for robots in human environments," *Control Engineering Practice*, vol. 34, pp. 376–385, 2007.

[12] C. Ott, A. Albu-Schäffer, A. Kugi, and G. Hirzinger, "Decoupling based cartesian impedance control of flexible joint robots," in *Proceedings of the IEEE International Conference on Robotics and Automation*, Taipei, Taiwan, 2003.

[13] C. Albrichsfeld, M. Svinin, and H. Tolle, "Learning approach to the active compliance control of multi-arm robots coupled through a flexible object," in *Proc. of 3rd European Control Conference*, 1995.

[14] B. Kim, S. Oh, h. Suh, and B. Yi, "A compliance control strategy for robot manipulators under unknown environment," *KSME International Journal*, vol. 14, pp. 1081–1088, February 2000.

[15] J. Slotine and W. Li, *Applied Nonlinear Control*. Upper Saddle River, NJ, USA: Pearson Prentice Hall, 1991.

[16] H. Seraji, "Adaptive compliance control: An approach to implicit force control in compliant motion," 1994. [Online]. Available: citeseer.ist.psu.edu/404588.html

[17] R. Colbaugh, H. Seraji, and K. Glass, "Adaptive compliant motion control for dextrous manipulators," *The International Journal of Robotic Research*, vol. 14, no. 3, pp. 270–280, 1995.

[18] R. Colbaugh, K. Glass, and K. Wedeward, "Adaptive compliance control of electrically-driven manipulators," in *Proceedings of the 35th Conference on Decision and Control*, Kobe,Japan, December 1996, pp. 394–399.

[19] R. Colbaugh, K. Wedeward, K. Glass, and H. Seraji, "New results on adaptive compliant motion control for dextrous manipulators," *The International Journal of Robotic and Automation*, vol. 11, no. 1, 1996.

[20] A. Spiers, G. Herrmann, and C. Melhuish, "Implementing discomfort in operational space: Practical application of a human motion inspired robot controller," *TAROS conference: Towards Autonomous Robotic Systems*, August 2009.

[21] A. Spiers, G. Herrmann, C. Melhuish, T. Pipe, and A. Lenz, ""Robotic Implementation of Realistic Reaching Motion using a Sliding Mode/Operational Space Controller,"," *Lecture Notes in Computer Science (ICSR '09)*, pp. 230–238, 2009.

[22] V. De Sapio, O. Khatib, and S. Delp, "Simulating the task level control of human motion: a methodology and framework for implementation," *The Visual Computer*, vol. 21, no. 5, pp. 289–302, 2005.

[23] G. Herrmann, M. Turner, and I. Postlethwaite, "Performance-oriented antwindup for a class of linear control systems with augmented neural network controller," *IEEE Transactions on Neural Networks*, vol. 18, no. 2, pp. 449–465, March 2007.

[24] S. Khan, G. Herrmann, A. Pipe, and C. Melhuish, "Safe adaptive compliance control of a humanoid robotic arm with anti-windup compensation and posture control," *Springer International Journal of Social Robotics(SORO)*, 2010.

[25] O. Khatib, "A unified approach for motion and force control of robot manipulators: The operational space formulation," *IEEE Journal of Robotics and Automation*, vol. RA3, no. 1, pp. 43–53, 1987.

[26] B. Nemec and L. Zlajpah, "Null space velocity control with dynamically consistent pseudo-inverse," *Robotica*, vol. 18, no. 1, p. 513518, 2000.